Title

Single-Cell Transcriptome Analysis Reveals Dynamic Cell Populations and Differential Gene Expression Patterns in Control and Aneurysmal Human Aortic Tissue.

Journal

Circulation, 142(14)

Authors

Li, Yanming

Ren, Pingping

Dawson, Ashley

et al.

Publication Date

2020-10-06

DOI

10.1161/CIRCULATIONAHA.120.046528

Peer reviewed

HHS Public Access

Author manuscript

Circulation. Author manuscript; available in PMC 2021 October 06.

Published in final edited form as:

Circulation. 2020 October 06; 142(14): 1374–1388. doi:10.1161/CIRCULATIONAHA.120.046528.

Single-cell Transcriptome Analysis Reveals Dynamic Cell Populations and Differential Gene Expression Patterns in Control and Aneurysmal Human Aortic Tissue

Yanming Li, PhD[1,2], **Pingping Ren, MD, PhD**[1,2], **Ashley Dawson, MD**[1,2], **Hernan G. Vasquez, PhD**[1,2], **Waleed Ageedi, MD**[1,2], **Chen Zhang, MD**[1,2], **Wei Luo, MD**[1,2], **Rui Chen, PhD**[3], **Yumei Li, PhD**[3], **Sangbae Kim, PhD**[3], **Hong S. Lu, MD, PhD**[4,5], **Lisa A. Cassis, PhD**[6], **Joseph S. Coselli, MD**[1,7,8], **Alan Daugherty, PhD**[4,5], **Ying H. Shen, MD PhD**[1,2,7,*], **Scott A. LeMaire, MD**[1,2,7,8,*]

[1]Division of Cardiothoracic Surgery, Michael E. DeBakey Department of Surgery, Baylor College of Medicine, Houston, TX, USA

[2]Department of Cardiovascular Surgery, Texas Heart Institute, Houston, TX, USA

[3]Human Genome Sequencing Center, Baylor College of Medicine, Houston, TX, USA

[4]Saha Cardiovascular Research Center, University of Kentucky, Lexington, KY, USA

[5]Department of Physiology, University of Kentucky, Lexington, KY, USA

[6]Department of Pharmacology and Nutritional Sciences, University of Kentucky, Lexington, KY

[7]Cardiovascular Research Institute, Baylor College of Medicine, Houston, TX, USA

[8]Department of Molecular Physiology and Biophysics, Baylor College of Medicine, Houston, TX, USA

Abstract

BACKGROUND: Ascending thoracic aortic aneurysm (ATAA) is caused by the progressive weakening and dilatation of the aortic wall and can lead to aortic dissection, rupture, and other life-threatening complications. To improve our understanding of ATAA pathogenesis, we sought to comprehensively characterize the cellular composition of the ascending aortic wall and to identify molecular alterations in each cell population of human ATAA tissues.

Correspondence: Scott A. LeMaire, MD, Michael E. DeBakey Department of Surgery, Baylor College of Medicine, One Baylor Plaza, BCM 390, Houston, Texas 77030. Phone: 832.355.9942; fax: 832.355.9928; slemaire@bcm.edu; or: Ying H. Shen, MD, PhD, Michael E. DeBakey Department of Surgery, Baylor College of Medicine, One Baylor Plaza, BCM 390, Houston, Texas 77030. Phone: 832.355.9952; fax: 832.355.9951; hyshen@bcm.edu.
*Co-senior authors

Disclosures

The authors report no conflicts of interest. Dr. LeMaire serves as a consultant for Terumo Aortic and Baxter Healthcare; serves as a principal investigator for clinical studies sponsored by Terumo Aortic and CytoSorbants; and serves as a co-investigator for clinical studies sponsored by W.L. Gore & Associates.

Supplemental Materials

Expanded Methods

Figures I-IX

Excel Files I-IV

References 41–49

METHODS: We performed single-cell RNA sequencing (sc-RNAseq) analysis of ascending aortic tissues from 11 study participants, including 8 patients with ATAA (4 women and 4 men) and 3 controls (2 women and 1 man). Cells extracted from aortic tissue were analyzed and categorized by using sc-RNAseq data to perform cluster identification. ATAA-related changes were then examined by comparing the proportions of each cell type and the gene expression profiles between ATAA and control tissues. We also examined which genes may be critical for ATAA by performing the integrative analysis of our sc-RNAseq data with publicly available data from genome-wide association studies (GWAS).

RESULTS: We identified 11 major cell types in human ascending aortic tissue; the high-resolution reclustering of these cells further divided them into 40 subtypes. Multiple subtypes were observed for smooth muscle cells, macrophages, and T lymphocytes, suggesting that these cells have multiple functional populations in the aortic wall. Generally, ATAA tissues had fewer nonimmune cells and more immune cells, especially T lymphocytes, than did control tissues. Differential gene expression data suggested the presence of extensive mitochondrial dysfunction in ATAA tissues. In addition, integrative analysis of our sc-RNAseq data with public GWAS data and promoter capture Hi-C data suggested that *ERG* (ETS [erythroblast transformation-specific] related gene) exerts an important role in maintaining normal aortic wall function.

CONCLUSIONS: Our study provides a comprehensive evaluation of the cellular composition of the ascending aortic wall and reveals how the gene expression landscape is altered in human ATAA tissue. The information from this study makes important contributions to our understanding of ATAA formation and progression.

Keywords

ascending thoracic aortic aneurysm; single-cell RNA sequencing; mitochondrial dysfunction; ERG

INTRODUCTION

Ascending thoracic aortic aneurysm (ATAA) is characterized by the weakening and dilatation of the ascending aorta, which can lead to dissection, rupture, and other life-threatening complications.[1,2] Although it has been well established that aortic degeneration marked by smooth muscle cell (SMC) loss and extracellular matrix (ECM) degradation is the main feature of ATAA, the molecular and cellular processes that lead to aortic degeneration in sporadic ATAA remain poorly understood.

The aortic wall consists of multiple cell types with various functions.[3] The heterogeneity of cell types is critical for aortic wall function. However, this heterogeneity of aortic cells has previously been neglected in experimental and bioinformatics studies, and precisely identifying the molecular changes in the ATAA wall is difficult when only pooled, tissue-level assays are used. Capturing cell-specific changes in the aortic wall from ATAA patients would profoundly improve our understanding of ATAA pathogenesis. A powerful tool for characterizing the expression of genes in individual cells is single-cell RNA sequencing (sc-RNAseq).[4–7] With its capacity for identifying cell-to-cell variability, sc-RNAseq can be used to reveal complex cell populations and uncover regulatory relationships between genes.[8–11]

In this study, we characterized the cellular heterogeneity of the human ascending aortic wall by performing sc-RNAseq. To comprehensively study molecular alterations in human ATAA tissues, we performed integrative and differential analysis of our sc-RNAseq data. Our analyses indicated that ATAA tissues have fewer nonimmune cells and more immune cells, especially T lymphocytes, than control aortic tissues and that ATAA tissues show evidence of extensive mitochondrial dysfunction. To reveal the genes that are potentially critical for ATAA, we integrated our sc-RNAseq data with public genome-wide association studies (GWAS) data and promoter capture Hi-C data. Our integrative analyses suggest that the gene *ERG* (ETS [erythroblast transformation-specific] related gene) plays an important role in maintaining aortic wall function. Overall, our study provides a comprehensive evaluation of the cellular composition of the human ascending aortic wall and reveals how the gene expression landscape is altered in the aortic wall of ATAAs.

METHODS

The data, analytic methods, and study materials will be made available to other researchers for the purposes of reproducing results or replicating procedures.

Enrollment of Study Participants and Collection of Tissue Samples

The protocol for collecting human tissue samples was approved by the Institutional Review Board at Baylor College of Medicine. Written informed consent was provided by all participants or the organ donors' legal representatives before enrollment. All experiments conducted with human tissue samples were performed in accordance with the relevant guidelines and regulations. Control ascending aortic tissue samples were obtained from recipients of heart transplants or lung donors, and diseased aortic tissue samples were obtained from patients with sporadic ATAA. Patients were excluded who had ascending aortic dissection, an heritable form of aortopathy (e.g., Marfan syndrome, Loeys-Dietz syndrome, a first-degree relative with ATAA, bicuspid aortic valve), or ATAA related to infection, aortitis, trauma, or isolated pseudoaneurysm. Detailed methods are provided in the Supplement.

Statistical Analysis

To examine whether a particular class of genes had increased (or decreased) expression in ATAA tissues, we used the Wilcox.test function of R to perform a one-sample Wilcoxon signed-rank test to test the hypothesis that the logFC across all genes was greater (or smaller) than 0.

RESULTS

Sc-RNAseq Analysis of Human Ascending Aortic Wall

We obtained nondiseased ascending aortic wall tissue from two heart transplant recipients and one lung donor, and aneurysmal ascending aortic wall tissue from eight ATAA patients (Table 1). A total of 48,128 qualified cells were obtained for further analysis (Figure 1A). For each sample, we performed individual data quality control and cell cluster identification

by using R package Seurat to obtain a preliminary estimate of the cell composition of each tissue sample (Figure I in the Supplement).

Gene Profiles of 11 Major Cell Types in Human Ascending Aortic Wall

Data from the 11 samples were then combined using Seurat. Integrative unsupervised cell clustering analysis was performed, and cells were projected onto a two-dimensional t-SNE plot. Initially, 24 clusters were obtained (Figure IIA in the Supplement). After examining conserved genes in each cluster (Figure IIB in the Supplement), we merged clusters with similar gene expression profiles and identified 11 major cell types in the ascending aortic wall (Figure 1A, B). The 11 major cell types included two clusters of SMCs, fibroblasts, mesenchymal stem cells (MSCs), endothelial cells (ECs), monocytes/macrophages/dendritic cells (DCs), T lymphocytes, natural killer (NK) cells, mast cells, B lymphocytes, and plasma cells (Figure 1B–D). Each cell type showed a distinct gene expression profile (Figure 1B, C).

Based on the top 2000 variable genes, we assigned these 11 cell types to one of two major groups: nonimmune cells or immune cells (Figure III in the Supplement). When we examined the source composition of each cell type (Figure 1E, Excel File I in the Supplement), we found that the three control tissues contributed more cells than expected in the nonimmune cell group, whereas the eight aneurysm tissues contributed more cells than expected in the immune cell group. This indicated the loss of nonimmune cells and the gain of immune cells in the ATAA wall, which is consistent with current knowledge.[3]

Nonimmune Cell Populations in Human Ascending Aortic Wall

Nonimmune cells have fundamental and critical roles in the aortic wall. To gain additional insight into nonimmune cells in the ascending aortic wall, we performed integrative unsupervised reclustering in all nonimmune cells (i.e., two clusters of SMCs, endothelial cells, fibroblasts, and MSCs) from ten tissues. One ATAA tissue sample (i.e., ATAA1) contained only 63 nonimmune cells, thereby making it technically difficult to merge with other datasets; therefore, it was excluded before additional analyses were performed in nonimmune cells. We obtained 15 types of nonimmune cells (Figure 2A–C) and renamed them according to their specific gene expression profiles (Figure 2B, C). In addition, to obtain a more comprehensive understanding of the types of nonimmune cells, we evaluated several features (or functions) (Figure 2D, Excel File II and III in the Supplement), as well as cell-cell and cell-ECM junction scores (Figure 2E, Excel File II and IV in the Supplement).

Heterogeneity of SMC Populations in Human Ascending Aortic Wall

Among the 15 types of nonimmune cells, we identified five SMC or SMC-related clusters. The Contractile SMC cluster highly expressed contraction-related genes such as *ACTC1*, *ACTA2*, and *MYL9* and the noncoding RNA *CARMN* (Figure 2B, C). It also expressed low levels of collagen and proteoglycan genes (Figure 2D) and had moderate cell-cell and cell-ECM junction scores (Figure 2E).

The cluster Stressed SMC shared several features with Contractile SMC, including expression of contraction-related genes, moderate cell-cell junction and cell-ECM junction scores, and low expression of ECM-related genes (Figure 2B–E). However, Stressed SMC also expressed stress response genes, such as *FOS*, *ATF3*, *JUN*, and *HSPB8*,[12] suggesting activation of the stress response in this type of SMC (Figure 2B, C).

The Proliferating SMC cluster showed higher cyclin gene expression and lower cell-cell junction scores than did the Contractile SMC cluster (Figure 2D, E), which was consistent with higher proliferation. We identified two types of SMCs in the Proliferating SMC cluster that both expressed contraction-related genes (Figure 2B, C) and low levels of collagen and proteoglycan genes (Figure 2C, D, Figure IVA, B in the Supplement). Interestingly, the Proliferating SMC cluster highly expressed synthetic SMC marker genes *MGP*, *TPM4*, and *MYH10*[13,14] (Figure 2C). However, unlike traditional synthetic SMCs, Proliferating SMC did not show low expression of contractile genes or elevated expression of ECM genes.

Fibromyocytes have properties of both fibroblasts and muscle cells.[15] The Fibromyocyte cluster expressed contractile genes, such as *ACTA2* and *MYL9*, and ECM genes, such as *COL1A2* and *COL8A1* (Figure 2B, C). Compared with the Contractile SMC cluster, the Fibromyocyte cluster showed similar contractile gene expression levels and cell-cell junction scores (Figure 2D, E). Furthermore, the Fibromyocyte cluster expressed higher levels of collagen and proteoglycan genes than did other SMC clusters but lower levels of these genes than did the Fibroblast cluster (Figure 2D, Figure IVA, B in the Supplement), in addition to a very high cell-ECM junction score (Figure 2E).

Fibroblasts and Other Nonimmune Cells in Human Ascending Aortic Wall

We identified two types of fibroblasts (i.e., clusters Fibroblast1 and Fibroblast2) that highly expressed collagen and proteoglycan genes, such as *COL1A2*,[16] *DCN*,[17] *LUM*, and *CLU* (Figure 2B, C). However, ECM mRNA abundance was slightly different between the Fibroblast1 and Fibroblast2 clusters (Figure IVA in the Supplement). For example, Fibroblast1 cells highly expressed elastin (*ELN*), whereas Fibroblast2 cells highly expressed fibrillin-1 (*FBN1*) and proteoglycans (e.g., *LUM* and *DCN*; Figure IVA in the Supplement). In addition, the Fibroblast1 cluster showed higher cell-cell and cell-ECM junction scores than did the Fibroblast2 cluster (Figure 2E), although not as high as the Contractile SMC cluster, suggesting that cell-cell and cell-ECM interactions occur in Fibroblast1 cells.

We identified two types of MSCs (i.e., clusters MSC1 and MSC2), which are sometimes referred to as pericytes,[18] that expressed the MSC marker genes *CSPG4* (NG2), *PDGFRB*, and *THY1* (CD90)[19,20] (Figure 2C). Cells in MSC clusters also moderately expressed cyclins (Figure 2D, Figure IVC in the Supplement), suggesting that they are more proliferative than cells in Contractile SMC and Fibroblast clusters. Cell-cell junction scores of MSC1 ranged from 0.6–6.9, whereas those of MSC2 ranged from 1.0–11.0. The cell-ECM junction score of MSC1 was 15.1, and that of MSC2 was 15.3. Cell-cell and cell-ECM junction scores suggested that minimal cell-cell or cell-ECM interactions occur in MSC clusters (Figure 2E). Interestingly, MSC1 expressed contraction-related genes (Figure 2B, C), whereas MSC2 expressed ECM genes (Figure IVA in the Supplement). Thus, in addition

to high proliferation and low junction, MSC1 may also participate in contraction, whereas MSC2 may be involved in ECM secretion.

We identified three small clusters of inflammatory cells (i.e., Inflammatory1, Inflammatory2, and Inflammatory3) that expressed cytokine and major histocompatibility complex (MHC) genes (Figure 2D, Figure IVD in the Supplement). Inflammatory1 showed a T lymphocyte–like gene expression profile (such as *CXCR4* and *CCL4*) (Figure 2C, Figure IVD in the Supplement), whereas Inflammatory2 expressed several macrophage-specific genes, such as *C1QA* and *C1QB*[21] (Figure 2C). Inflammatory3 expressed interferon-induced genes such as *IFIT1* and *IFI6* (Figure 2C).

We identified two clusters of endothelial cells (i.e., EC1 and EC2) that expressed endothelial marker genes *VWF*, *PECAM1*,[17] and *IFI27* (Figure 2B, C) and had a high cell-cell junction score with other endothelial cells (Figure 2E). EC2 showed higher cell-cell (junction scores of EC1-EC1: 41.8, EC1-EC2: 54.7, EC2-EC2: 92.0) and cell-ECM junction scores (cell-ECM scores of EC1 is 14.5, EC2 is 19.2) than did EC1 (Figure 2E), which may suggest greater cell motility or cell migration for EC1.

A small cluster of Schwann cells was identified that expressed *NGFR*[22] (Figure 2C). These cells had a high cell-cell junction score with other Schwann cells (Figure 2E).

Dynamic Monocyte/Macrophage/DC Cluster in Human Ascending Aortic Wall

The monocyte/macrophage/DC cluster showed a heterogeneous distribution in the t-SNE plot. We performed integrative unsupervised reclustering of the monocyte/macrophage/DC population from all 11 ascending aortic tissue samples. Initially, we obtained 14 clusters. After examining conserved genes in each cluster (Figure V in the Supplement), we merged clusters with similar gene expression profiles and obtained ten types of monocyte/macrophage/DCs (Figure 3A–D).

Expression analysis of well-defined M1 and M2 marker genes in each cluster demonstrated that M1 marker genes *TNF*, *IL1B*, and *NFKB1*[23,24] were highly expressed in 2 of 3 M1-like clusters, whereas M2 marker genes *MERTK*, *MRC1*, *STAB1*, and *CD163*[23,24] were highly expressed in all M2-like clusters (Figure 3B, C).

The M1like1 cluster expressed several cytokine genes, including *CCL3L1*, *CCL4L2*, *CCL4*, and *TNF* (Figure 3E), indicating an inflammatory function. In addition to expressing M1 marker genes, M1like2 cells expressed epidermal growth factor–encoding genes *EREG* and *AREG*, metalloproteinase inhibitor–encoding gene *TIMP1*, and chondroitin sulfate proteoglycan–encoding gene *VCAN* (Figure 3D), suggesting that this type of M1-like macrophage may be involved in tissue remodeling, in addition to secreting inflammatory factors. The M1like3 cluster expressed transcription factor–encoding genes such as *ETS1* and *RUNX3* (Figure 3D). M1like3 cells also expressed genes encoding MHC class I molecules, which specifically present antigens to cytotoxic CD8 T lymphocytes,[25] whereas other macrophages primarily expressed genes encoding MHC class II molecules (Figure 3E). This suggested that M1like3 cells present antigens to CD8 T lymphocytes rather than to CD4 T lymphocytes.

The M2like1 cluster expressed *PDK4*, *STAB1*, *TXNIP*, and *MAF* (Figure 3E), suggesting roles in glucose metabolism, anti-inflammation, and phagocytosis. Conserved genes in M2like2 included *C1QA*, *C1QB*, *C1QC*, and *RAB13*, which were mostly also expressed in M2like1 (Figure 3D). However, several M2like1-specific genes were not expressed in M2like2 cells (Figure 3D). The M_IFNresponse cluster expressed many interferon-induced genes including *IFI44L*, *ISG15*, *IFIT1*, and *IFITM3* (Figure 3D). The M_remodeling cluster expressed several SMC or fibroblast genes including *IGFBP7*, *ADIRF*, *DSTN*, *TPM2*, *MGP*, and *MYL9* (Figure 3D), as well as several protease genes including *ADAMTS1*, *MMP2*, and *CTSF* (Figure 3E), suggesting a role in tissue remodeling. Finally, the M_Proliferating cluster expressed histone-related genes *H2AFZ*, *HMGB2*, and *HMGN2*; microtubule-related genes *TUBB*, *TUBA1B*, and *STMN*; and cyclin-dependent kinases regulatory subunit 1 *CKS1B* (Figure 3D).

The Monocyte cluster expressed *NAMPT*, *S100A9*, and *LITAF* (Figure 3D) and several cytokine receptor genes including *IL4R*, *CXCR1*, *IL1R1*, *IL10RA*, and *IL10RB* (Figure 3E). The high expression of receptor genes allowed monocytes to receive signals to start differentiating into either macrophages or DCs. The DC cluster expressed *FLT3*, *IRF8*, and *CLEC9A* (Figure 3D), as well as high levels of MHC genes (Figure 3E), which is in agreement with the identity of DCs as professional antigen-presenting cells.

T Lymphocytes in Human Ascending Aortic Wall

T lymphocytes were the largest cell population identified in ascending aortic tissues. To gain further insight, we combined all of the T lymphocytes from all 11 tissues and performed integrative unsupervised re-clustering. We obtained 11 clusters (Figure 3F). Based on the expression of CD4, CD8A, and CD8B, as well as the expression of the conserved genes in each cluster (Figure 3G, H), we renamed the T lymphocyte subclusters.

Active CD4 T lymphocytes (CD4_active) expressed *CREM*, *CXCR6*, *RGCC*, *MR3C1*, and *GZMB* (Figure 3G), indicating pro-inflammatory and cytotoxic functions. Resting CD4 T (CD4_EM_rest [effector memory rest CD4 T lymphocyte]) cells expressed *CCR7*, *IL7R*, *CCL20*, and *KLRB1* (Figure 3G). Regulatory CD4 T lymphocytes (CD4_Treg) expressed Treg-defining genes *IL2RA* and *CTLA4*, as well as *TNFRSF18*, *ID3*, and *LTB* (Figure 3G). In addition, CD4_Treg highly expressed several cytokine genes, especially cytokine receptor genes (e.g., *TFNAR2*, *TNFRSF9*, *CCR6*, and *IL2RA*), suggesting that cytokines may play an important role in Treg functionality (Figure 3I).

Active CD8 T lymphocytes (CD8_active) expressed cytotoxicity-associated genes *GZMK* and *CRTAM*, inflammatory gene *CCL4*, as well as *CMC1* (Figure 3G). CD8 terminally differentiated effector T lymphocytes (CD8_TEMRA) expressed cytotoxic genes *GNLY*, *KLRD1*, and *PRF1*, as well as *CCL5* and *HOPX* (Figure 3G).

The T_HSP cluster contained both CD4 and CD8 T lymphocytes (Figure 3G, H) and highly expressed stress response genes, including *JUN*, *FOS*, and genes encoding heat shock proteins (HSPs), including *HSPA1A*, *HSPA1B*, and *HSP90AA1* (Figure 3G). The T_GIMAP cluster also contained both CD4 and CD8 T lymphocytes. T_GIMAP cells expressed GTPase of the immunity associated protein family genes, including *GIMAP1*,

GIMAP4, and *GIMAP7*, and lncRNA *MALAT1* (Figure 3G). Both T_HSP and T_GIMAP clusters expressed *TXNIP* (Figure 3G), which encodes a protein that inhibits the antioxidative function of thioredoxin, resulting in the accumulation of reactive oxygen species and cellular stress.[26] The small T_stress cluster also expressed stress-related genes such as *JUN*, *FOS*, and *DNAJA1*. The T_proliferation cluster expressed microtubule-related genes *TUBA1B* and *STMN1*, chromatin-associated non-histone protein genes *HMGB1* and *HMGN2*, and *CKS1B*, encoding cyclin-dependent kinases regulatory subunit 1 (Figure 3G). T_switched cells expressed the contraction--related genes *TAGLN*, *MYH11*, and *TPM1* (Figure 3G).

Similar Stress Response in Select Cell Types

After clustering and reclustering, a total of 40 cell types were identified in the ascending aortic tissue (Figure VIA in the Supplement). We noticed that *JUN*, *FOS*, and HSP genes were identified as conserved marker genes for the Stressed SMC, T_HSP, and T_stress clusters. Previously, O'Flanagan et al[12] reported that tissue dissociation with collagenase at 37°C triggers induction of stress response genes, including *JUN*, *FOS*, and HSP. When we calculated the total expression of the top 40 tissue dissociation–induced genes,[12] the Stressed SMC, T_stress, and T_HSP clusters showed higher total expression of dissociation-induced genes than did other clusters (Figure VIB in the Supplement). Thus, the gene expression profiles for these three clusters may not truly represent their physiologic molecular status.

Phenotype Switch Between Major Cell Types

Three small nonimmune cell clusters (Inflammatory1, Inflammatory2, and Inflammatory3) showed immune cell expression profiles. The M_remodelling cluster expressed SMC and fibroblast genes, whereas the T_switched cluster expressed contraction-related genes. Previous studies have shown the plasticity of SMCs.[27,28] Trajectory analysis indicated that Contractile SMC possesses the potency to redifferentiate towards Inflammatory2 and M_remodelling in one direction and towards Inflammatory1 and T_switched in another direction (Figure VII in the Supplement).

Decreased Mitochondrial Function in ATAA Tissues

To identify key changes in ATAA tissues, we compared data between ATAA and control tissues and performed differential analysis by cell type (Figure 4A–D). Of the 40 clusters, 14 showed more than 500 differentially expressed genes (Figure 4A, left panel). GSEA indicated that oxidative phosphorylation (OXPHOS) was increased in seven clusters in ATAA tissues (Figure 4B). However, although mitochondria are the main organelle for OXPHOS, the expression of mitochondrial genes was decreased in several cell types (Figure 5A). Analysis of all 97 genes that encoded OXPHOS complexes showed that mitochondrial OXPHOS gene expression decreased, whereas chromatin OXPHOS gene expression increased in many cell types in ATAA tissues (Figure 4C, Figure VIIIA in the Supplement). Further examination of the fold change for each gene by cell type showed that 24/40 cell types in ATAA tissues had significantly decreased mitochondrial gene expression and increased chromatin OXPHOS gene expression (Figure 4C). Therefore, we hypothesized that cells in ATAA tissues may exhibit mitochondrial dysfunction. When mitochondrial gene

expression is inhibited, chromatin OXPHOS gene expression may increase to compensate and maintain critical OXPHOS function in cells. The Stressed SMC cluster, one of the clusters containing cells that consume most of the ATP in the human aortic wall, showed increased glycolysis-related gene expression in ATAA tissues (Figure 4B), further suggesting that OXPHOS ATP production may not be sufficient for SMC contractile activities.

Elevated Chemokine Expression in Nonimmune Cells and Macrophages in ATAA Tissues

Compared with control tissues, ATAA tissues showed a decreased proportion of most nonimmune cells and an increased proportion of immune cells, especially T lymphocytes (Figure 4A, right panel), which is consistent with our analysis of cell composition (Figure 1E).

Cell cycle analysis indicated more cells were assigned to the G1 stage in ATAA tissues than in control tissues (Figure VIIIB in the Supplement), which indicated a lower proliferation rate in ATAA tissues. This also suggested that the increased proportion of T lymphocytes in ATAA tissues may not arise from cell proliferation.

We calculated the fold change (i.e., ATAA/control) of all chemokine genes according to cell type and identified 23 clusters with significantly increased chemokine gene expression in ATAA tissues (Figure 4D). Among the 23 clusters, 12 were nonimmune cells, and 4 were macrophages. This suggested that the altered cell population in ATAA may primarily be attributed to elevated chemokine expression in nonimmune cells and macrophages, which attracts distal immune cells.

Association of Differentially Expressed Genes in ATAA Tissues with GWAS Results

Thousands of DEGs were identified between ATAA and control tissues. However, some of those DEGs may have arisen from other cofounding factors such as tissue processing, and some DEGs may not be involved in ATAA directly. We sought to identify DEGs that are involved in ATAA initiation and development, which may help us understand the pathogenesis of ATAA and develop potential treatments.

GSEA chromatin position enrichment analysis of all DEGs indicated that 4 chromatin regions and a mitochondrial region were enriched with DEGs (Figure 5A). We further used the results of GWAS studies to extract all aneurysm-related SNPs, as well as the chromatin regions of those SNPs. All 4 chromatin regions that were enriched with DEGs harbored aneurysm-associated SNPs (Figure IXA in the Supplement). In addition, we calculated the distance from the chromatin regions with enriched DEGs to the aneurysm-associated SNPs and found that DEGs were physically closer to aneurysm-associated SNPs than were random genes (Figure 5B).

In a study by Jung et al,[29] putative target genes for GWAS SNPs were identified through promoter capture Hi-C data from 27 human cell and tissue types. From these data, we extracted putative target genes of aneurysm-associated SNPs and overlapped them with our DEGs. From these putative target genes of aneurysm-associated SNPs, we identified 11 genes (i.e., *TWIST1*, *ADAM15*, *ERG*, *UBE2Q1*, *TPM3*, *ATP8B2*, *C1orf43*, *RSAD2*,

DNM2, *KANK2*, and *HAX1*) that were differentially expressed in 16 cell types between control and ATAA tissues (Figure 5C). Of the 11 genes, *TWIST1* and *ERG* are two transcription factor–encoding genes. *ERG* was shown to be highly expressed in the aorta among 54 human cell and tissue types reported in the GTEx portal (Figure IXB in the Supplement). *ERG* was identified as a putative target gene of the aneurysm-associated SNP rs2836411.[30,31] Rs2836411 is an eQTL (expression quantitative trait loci) of *ERG*, and its risk allele is associated with decreased *ERG* expression.[31] We found that *ERG* expression was decreased in the clusters Proliferating SMC1, Proliferating SMC2, Inflammatory1, Fibroblast1, and EC1 (Figure 5D). To further identify potential target genes regulated by ERG in these five clusters, we intersected ERG target genes identified in other studies with DEGs by cluster. The initial ERG targets identified with ChIP-seq in human aortic endothelial cells were obtained from ChIP-Atlas (https://chip-atlas.org/). After those genes were intersected with DEGs in EC1, 149 genes (n=105 downregulated, n=44 upregulated in ATAA) were identified as genes potentially regulated by ERG in EC1 (Figure 5E). Gene Ontology (GO) analysis indicated that several genes downregulated in EC1 were involved in apoptosis, the response to reactive oxygen species, and ER signaling (Figure 5E). For the other four clusters, no ERG ChIP-seq data are available in corresponding cell types, so we intersected DEGs with predicted targets of ERG (obtained from http://tfbsdb.systemsbiology.net/). We identified 18 genes in Fibroblast1 (Figure 5F) and 6 genes in Proliferating SMC2 (Figure 5G) that are potentially regulated by ERG. Together, these findings indicate that ERG may be critical for the normal physiology of the aortic wall and play a critical role in SMCs, endothelial cells, and fibroblasts.

DISCUSSION

The present study revealed the comprehensive cellular composition of the human ascending aortic wall and provided novel insight into how the gene expression landscape is altered in different types of ATAA cells. Our data suggest that extensive mitochondrial dysfunction may occur in ATAA and that the gene *ERG* may play an important role that provides protection against aneurysm formation in SMCs, endothelial cells, and fibroblasts.

Our cellular composition data showed that there are four subtypes of SMCs and four types of SMC-related cells in the ascending aorta (i.e., fibromyocytes and three clusters of inflammatory nonimmune cells). The Proliferating SMC cluster expressed several synthetic marker genes, but it expressed high levels of contractile genes and low levels of ECM genes. These cells may play an adaptive role in aorta with their contractile function and high proliferation. Fibromyocytes are fibroblast-like cells that originate from SMCs.[15] Our data were not sufficient for tracing the origin of the Fibromyocyte cluster cells but suggested that they were SMCs with ECM features rather than fibroblasts with contractile features. Through trajectory analysis, we showed that SMCs possessed the potential to redifferentiate into inflammatory cells. Together, our data suggested that the potential various roles of SMCs primarily rely on their plasticity.

T lymphocytes are known for having many subtypes. We did not detect all the typical T lymphocyte subtypes in our analysis but did identify several atypical T lymphocyte subtypes such as T_IFNresponse, T_HSP, and T_GIMAP. The interferon response was observed in a

small group of T lymphocytes, as well as in a small group of macrophages and nonimmune cells, suggesting that viral infection may have been present in some of our study participants.[32] This finding, together with the possibility that the T_HSP subtype may have resulted from tissue processing, suggests that T lymphocytes can respond quickly to external stimuli in an atypical way.

Unexpectedly, our data suggested the presence of extensive mitochondrial dysfunction in many cell types within ATAA tissues. Because all the ATAA samples came from patients with advanced-stage disease that required surgery, it is likely that these patients had progressing ATAA for many years. Presumably, this would have created an environment of stress for aortic cells that, over time, would continue to weaken the aortic wall. Mitochondrial dysfunction has been associated with aging and chronic diseases,[33,34] supporting the notion that the long-term presence of ATAA may impair mitochondrial function.

Using sc-RNAseq, we identified genes that were differentially expressed in the aorta of patients with ATAA. We then integrated genes that were differentially expressed in ATAA tissues with GWAS results (aneurysm-associated SNPs) and used capture Hi-C data to determine their putative target genes. Specifically, we found that the transcription factor ERG may play a role in SMCs, endothelial cells, and fibroblasts that serves to maintain aortic wall function. Previous studies have suggested that ERG inhibits vascular inflammation in endothelial cells[35] and that reduced ERG expression is associated with aneurysms.[31] Furthermore, mechanistic studies have shown that ERG binds super enhancers in endothelial cells[36] and interacts with phosphorylated SMAD2 and SMAD3 in prostate cells.[37] We have also identified genes by cell type that are potentially regulated by ERG. *CFLAR*, *TNFAIP3*, and *GSK3B*, reported previously as apoptosis inhibitors,[38,39] were identified as targets of ERG and were downregulated in EC1. Another potential target gene, *TMEM173,* which encodes the cytosolic DNA sensing adaptor STING, was upregulated in the Fibroblast 1 cluster. Notably, *Sting*-deficient mice have reduced aortic enlargement, dissection, and rupture.[40] Together, our findings suggest that ERG may play a role in maintaining normal aortic function by positively regulating anti-apoptosis genes and negatively regulating pro-inflammatory genes in a direct manner.

In this study, we integrated sc-RNAseq datasets from 8 ATAA samples and 3 nonaneurysm control samples. The smaller sample size of the control group than the ATAA group may limit the statistical power of this comparison. Furthermore, two control samples came from heart transplant recipients. Thus, although those patients did not have aortic aneurysms, they may have exhibited molecular or cellular changes in the ascending aorta related to their cardiac disease. Additionally, the ethnicity and race of ATAA and control groups were not well matched. All ATAA patients were non-Hispanic white, whereas the control patients were more diverse with respect to ethnicity and race (Table 1). The inherent limitations related to using control specimens from transplant recipients not matched on the basis of ethnicity and race may weaken our comparative analysis findings. Additional control specimens from various sources should be assessed in subsequent studies to address these limitations. Of note, we have compared the control samples used in this study with control samples from five younger heart transplant donors (four who were non-Hispanic white) and

found that the two controls sets were similar in gene expression pattern, as well as in cellular composition compared with ATAA samples (data not shown), which suggests the reliability of the control specimens in our study.

To obtain a single-cell suspension for sequencing, we used an enzyme cocktail to digest the aortic wall. However, the recovery rate of each cell type was not equal. This recovery bias may be attributed to cell properties or distribution (e.g., the media may be harder to digest than the adventitia). Alternatively, some types of cells may be vulnerable to the digestion process, resulting in increased cell loss. Therefore, our data may not represent the actual proportion of cells in the human aortic wall. One potential solution for the recovery bias observed would be to digest the intima, media, and adventitia of the aorta separately and adjust the processing times according to each layer's susceptibility to the digestion enzyme cocktail.

Because the aortic wall is composed of compact tissue, extensive effort is required to obtain a single-cell suspension. The tissue digestion process can take 2 hours or longer. Our analysis revealed three cell types that were profoundly affected by tissue processing, although other cell types may have been affected to a lesser extent. Because control tissues have a healthier tissue status, they generally need more time to digest. GSEA of DEGs indicated that "TNFA signaling via NFKB" was decreased extensively in all ATAA cell types (Figure 4B). Notably, "TNFA signaling via NFKB" has been reported to be the most highly enriched function for genes induced by tissue processing,[12] suggesting that the decreased "TNFA signaling via NFKB" in ATAA tissues may have resulted from the shorter tissue-processing time. Indeed, the expression of the top genes triggered by tissue processing was higher in control tissues than in ATAA tissues for many cell types (Figure VIB in the Supplement). The stress response is an important molecular and cellular reaction that affects not only cell fate but the status of regional tissue. However, we are unable to dissect the physiologic stress response in ATAA tissues. Eliminating the influence of tissue processing is difficult, but it is possible to use the same duration of time for processing control and aneurysmal tissues to minimize the influence of tissue processing on the comparison between ATAA and control tissues.

Despite these limitations and technical challenges, our study yielded several interesting and novel findings. We revealed the cellular and molecular landscape of human ascending aortic wall at the single-cell level, and our data provide molecular profiles of multiple subtypes of aortic SMCs, macrophages, and T lymphocytes. Furthermore, the results of our comparative analyses suggest the presence of extensive mitochondrial dysfunction in ATAA tissues and indicate a potentially critical role for the gene *ERG* in protecting the aorta against ATAA. These findings expand our understanding of ATAA pathogenesis and may contribute to the development of new treatments.

Supplementary Material

Refer to Web version on PubMed Central for supplementary material.

Acknowledgments

We gratefully acknowledge Nicole Stancel, PhD, ELS(D), of Scientific Publications at the Texas Heart Institute, for editorial support. We also acknowledge Alon R. Azares, BS, at the Texas Heart Institute Flow Cytometry Core, for fluorescence-activated cell sorting support.

Sources of Funding

The research was supported by grants from the American Heart Association (AHA) Vascular Diseases Strategically Focused Research Networks (SFRN) (AHA18SFRN33960114, AHA18SFRN33960163, and AHA18SFRN33960253). Single-cell RNAseq was performed at the Single Cell Genomics Core at Baylor College of Medicine partially supported by NIH shared instrument grants (S10OD018033, S10OD023469, S10OD025240) and P30EY002520 to Rui Chen. Dr. Dawson is supported by a fellowship award through the University of Kentucky-Baylor College of Medicine Aortopathy Research Center within the AHA SFRN (18SFRN33960114). Dr. Ageedi is supported by the National Institutes of Health (NIH)/National Heart, Lung, and Blood Institute (NHLBI) T32 Research Training Program in Cardiovascular Surgery (T32-HL139430). Dr. LeMaire's work is supported in part by the Jimmy and Roberta Howell Professorship in Cardiovascular Surgery at Baylor College of Medicine.

Non-standard Abbreviations and Acronyms:

ATAA	ascending thoracic aortic aneurysm
DCs	dendritic cells
ECM	extracellular matrix
ECs	endothelial cells
eQTL	expression quantitative trait loci
ERG	ETS [erythroblast transformation-specific] related gene
GO	gene ontology
GWAS	genome-wide association studies
MSCs	mesenchymal stem cells
NK	natural killer
OXPHOS	oxidative phosphorylation
sc-RNAseq	single-cell RNA sequencing
SMC	smooth muscle cell

References

1. Lavall D, Schafers HJ, Bohm M, Laufs U. Aneurysms of the ascending aorta. Dtsch Arztebl Int. 2012;109:227–233. [PubMed: 22532815]
2. Goldfinger JZ, Halperin JL, Marin ML, Stewart AS, Eagle KA, Fuster V. Thoracic aortic aneurysm and dissection. J Am Coll Cardiol. 2014;64:1725–1739. [PubMed: 25323262]
3. Shen YH, LeMaire SA. Molecular pathogenesis of genetic and sporadic aortic aneurysms and dissections. Curr Probl Surg. 2017;54:95–155. [PubMed: 28521856]
4. Kolodziejczyk AA, Kim JK, Svensson V, Marioni JC, Teichmann SA. The technology and biology of single-cell RNA sequencing. Mol Cell. 2015;58:610–620. [PubMed: 26000846]

5. Zappia L, Phipson B, Oshlack A. Exploring the single-cell RNA-seq analysis landscape with the scRNA-tools database. PLoS Comput Biol. 2018;14:e1006245. [PubMed: 29939984]
6. Chen G, Ning B, Shi T. Single-cell RNA-seq technologies and related computational data analysis. Front Genet. 2019;10:317. [PubMed: 31024627]
7. Liu S, Trapnell C. Single-cell transcriptome sequencing: recent advances and remaining challenges. F1000Res. 2016;5.
8. Lukowski SW, Patel J, Andersen SB, Sim SL, Wong HY, Tay J, Winkler I, Powell JE, Khosrotehrani K. Single-cell transcriptional profiling of aortic endothelium identifies a hierarchy from endovascular progenitors to differentiated cells. Cell Rep. 2019;27:2748–2758 e2743. [PubMed: 31141696]
9. Cochain C, Vafadarnejad E, Arampatzi P, Pelisek J, Winkels H, Ley K, Wolf D, Saliba AE, Zernecke A. Single-cell RNA-seq reveals the transcriptional landscape and heterogeneity of aortic macrophages in murine atherosclerosis. Circ Res. 2018;122:1661–1674. [PubMed: 29545365]
10. Dobnikar L, Taylor AL, Chappell J, Oldach P, Harman JL, Oerton E, Dzierzak E, Bennett MR, Spivakov M, Jorgensen HF. Publisher Correction: Disease-relevant transcriptional signatures identified in individual smooth muscle cells from healthy mouse vessels. Nat Commun. 2018;9:5401. [PubMed: 30559342]
11. Baron CS, Kester L, Klaus A, Boisset JC, Thambyrajah R, Yvernogeau L, Kouskoff V, Lacaud G, van Oudenaarden A, Robin C. Single-cell transcriptomics reveal the dynamic of haematopoietic stem cell production in the aorta. Nat Commun. 2018;9:2517. [PubMed: 29955049]
12. O'Flanagan CH, Campbell KR, Zhang AW, Kabeer F, Lim JLP, Biele J, Eirew P, Lai D, McPherson A, Kong E, et al. Dissociation of solid tumor tissues with cold active protease for single-cell RNA-seq minimizes conserved collagenase-associated stress responses. Genome Biol. 2019;20:210. [PubMed: 31623682]
13. Beamish JA, He P, Kottke-Marchant K, Marchant RE. Molecular regulation of contractile smooth muscle cell phenotype: implications for vascular tissue engineering. Tissue Eng Part B Rev. 2010;16:467–491. [PubMed: 20334504]
14. Abouhamed M, Reichenberg S, Robenek H, Plenz G. Tropomyosin 4 expression is enhanced in dedifferentiating smooth muscle cells in vitro and during atherogenesis. Eur J Cell Biol. 2003;82:473–482. [PubMed: 14582535]
15. Wirka RC, Wagh D, Paik DT, Pjanic M, Nguyen T, Miller CL, Kundu R, Nagao M, Coller J, Koyano TK, et al. Atheroprotective roles of smooth muscle cell phenotypic modulation and the TCF21 disease gene as revealed by single-cell analysis. Nat Med. 2019;25:1280–1289. [PubMed: 31359001]
16. Ghosh AK, Yuan W, Mori Y, Varga J. Smad-dependent stimulation of type I collagen gene expression in human skin fibroblasts by TGF-beta involves functional cooperation with p300/CBP transcriptional coactivators. Oncogene. 2000;19:3546–3555. [PubMed: 10918613]
17. Zhang H, Tian L, Shen M, Tu C, Wu H, Gu M, Paik DT, Wu JC. Generation of quiescent cardiac fibroblasts from human induced pluripotent stem cells for in vitro modeling of cardiac fibrosis. Circ Res. 2019;125:552–566. [PubMed: 31288631]
18. Crisan M, Yap S, Casteilla L, Chen CW, Corselli M, Park TS, Andriolo G, Sun B, Zheng B, Zhang L, et al. A perivascular origin for mesenchymal stem cells in multiple human organs. Cell Stem Cell. 2008;3:301–313. [PubMed: 18786417]
19. Tian X, Brookes O, Battaglia G. Pericytes from mesenchymal stem cells as a model for the blood-brain barrier. Sci Rep. 2017;7:39676. [PubMed: 28098158]
20. Michelis KC, Nomura-Kitabayashi A, Lecce L, Franzen O, Koplev S, Xu Y, Santini MP, D'Escamard V, Lee JTL, Fuster V, et al. CD90 identifies adventitial mesenchymal progenitor cells in adult human medium- and large-sized arteries. Stem Cell Reports. 2018;11:242–257. [PubMed: 30008326]
21. Fraser DA, Laust AK, Nelson EL, Tenner AJ. C1q differentially modulates phagocytosis and cytokine responses during ingestion of apoptotic cells by human monocytes, macrophages, and dendritic cells. J Immunol. 2009;183:6175–6185. [PubMed: 19864605]

22. Ratner N, Williams JP, Kordich JJ, Kim HA. Schwann cell preparation from single mouse embryos: analyses of neurofibromin function in Schwann cells. Methods Enzymol. 2006;407:22–33. [PubMed: 16757311]
23. Chinetti-Gbaguidi G, Colin S, Staels B. Macrophage subsets in atherosclerosis. Nat Rev Cardiol. 2015;12:10–17. [PubMed: 25367649]
24. Raffort J, Lareyre F, Clement M, Hassen-Khodja R, Chinetti G, Mallat Z. Monocytes and macrophages in abdominal aortic aneurysm. Nat Rev Cardiol. 2017;14:457–471. [PubMed: 28406184]
25. Kornum BR, Knudsen S, Ollila HM, Pizza F, Jennum PJ, Dauvilliers Y, Overeem S. Narcolepsy. Nature Reviews Disease Primers. 2017;3:16100.
26. Yoshihara E, Masaki S, Matsuo Y, Chen Z, Tian H, Yodoi J. Thioredoxin/Txnip: redoxisome, as a redox switch for the pathogenesis of diseases. Front Immunol. 2014;4:514. [PubMed: 24409188]
27. Rong JX, Shapiro M, Trogan E, Fisher EA. Transdifferentiation of mouse aortic smooth muscle cells to a macrophage-like state after cholesterol loading. Proc Natl Acad Sci U S A. 2003;100:13531–13536. [PubMed: 14581613]
28. Clement M, Chappell J, Raffort J, Lareyre F, Vandestienne M, Taylor AL, Finigan A, Harrison J, Bennett MR, Bruneval P, et al. Vascular Smooth Muscle Cell Plasticity and Autophagy in Dissecting Aortic Aneurysms. Arterioscler Thromb Vasc Biol. 2019;39:1149–1159. [PubMed: 30943775]
29. Jung I, Schmitt A, Diao Y, Lee AJ, Liu T, Yang D, Tan C, Eom J, Chan M, Chee S, et al. A compendium of promoter-centered long-range chromatin interactions in the human genome. Nat Genet. 2019;51:1442–1449. [PubMed: 31501517]
30. Jones GT, Tromp G, Kuivaniemi H, Gretarsdottir S, Baas AF, Giusti B, Strauss E, Van't Hof FN, Webb TR, Erdman R, et al. Meta-analysis of genome-wide association studies for abdominal aortic aneurysm identifies four new disease-specific risk loci. Circ Res. 2017;120:341–353. [PubMed: 27899403]
31. Marsman J, Gimenez G, Day RC, Horsfield JA, Jones GT. A non-coding genetic variant associated with abdominal aortic aneurysm alters ERG gene regulation. Hum Mol Genet. 2019:554–565.
32. Perry AK, Chen G, Zheng D, Tang H, Cheng G. The host type I interferon response to viral and bacterial infections. Cell Res. 2005;15:407–422. [PubMed: 15987599]
33. Pieczenik SR, Neustadt J. Mitochondrial dysfunction and molecular pathways of disease. Exp Mol Pathol. 2007;83:84–92. [PubMed: 17239370]
34. Lin MT, Beal MF. Mitochondrial dysfunction and oxidative stress in neurodegenerative diseases. Nature. 2006;443:787–795. [PubMed: 17051205]
35. Sperone A, Dryden NH, Birdsey GM, Madden L, Johns M, Evans PC, Mason JC, Haskard DO, Boyle JJ, Paleolog EM, et al. The transcription factor Erg inhibits vascular inflammation by repressing NF-kappaB activation and proinflammatory gene expression in endothelial cells. Arterioscler Thromb Vasc Biol. 2011;31:142–150. [PubMed: 20966395]
36. Kalna V, Yang Y, Peghaire CR, Frudd K, Hannah R, Shah AV, Osuna Almagro L, Boyle JJ, Gottgens B, Ferrer J, et al. The transcription factor ERG regulates super-enhancers associated with an endothelial-specific gene expression program. Circ Res. 2019;124:1337–1349. [PubMed: 30892142]
37. Fang J, Xu H, Yang C, Morsalin S, Kayarthodi S, Rungsrisuriyachai K, Gunnal U, McKenzie B, Rao VN, Reddy ES. Ets related gene and Smad3 proteins collaborate to activate transforming growth factor-beta mediated signaling pathway in ETS related gene-positive prostate cancer cells. J Pharm Sci Pharmacol. 2014;1:175–181. [PubMed: 25745638]
38. De Valck D, Jin DY, Heyninck K, Van de Craen M, Contreras R, Fiers W, Jeang KT, Beyaert R. The zinc finger protein A20 interacts with a novel anti-apoptotic protein which is cleaved by specific caspases. Oncogene. 1999;18:4182–4190. [PubMed: 10435631]
39. Beurel E, Jope RS. The paradoxical pro- and anti-apoptotic actions of GSK3 in the intrinsic and extrinsic apoptosis signaling pathways. Prog Neurobiol. 2006;79:173–189. [PubMed: 16935409]
40. Luo W, Wang Y, Zhang L, Ren P, Zhang C, Li Y, Azares AR, Zhang M, Guo J, Ghaghada KB, et al. Critical Role of Cytosolic DNA and Its Sensing Adaptor STING in Aortic Degeneration, Dissection, and Rupture. Circulation. 2020;141:42–66. [PubMed: 31887080]

41. Stuart T, Butler A, Hoffman P, Hafemeister C, Papalexi E, Mauck WM 3rd, Hao Y, Stoeckius M, Smibert P, Satija R. Comprehensive integration of single-cell data. Cell. 2019;177:1888–1902 e1821. [PubMed: 31178118]
42. Risso D, Perraudeau F, Gribkova S, Dudoit S, Vert JP. A general and flexible method for signal extraction from single-cell RNA-seq data. Nat Commun. 2018;9:284. [PubMed: 29348443]
43. McCarthy DJ, Chen Y, Smyth GK. Differential expression analysis of multifactor RNA-Seq experiments with respect to biological variation. Nucleic Acids Res. 2012;40:4288–4297. [PubMed: 22287627]
44. Yu G, Wang LG, Han Y, He QY. clusterProfiler: an R package for comparing biological themes among gene clusters. OMICS. 2012;16:284–287. [PubMed: 22455463]
45. Sergushichev AA. An algorithm for fast preranked gene set enrichment analysis using cumulative statistic calculation. bioRxiv. 2016.
46. Qiu X, Hill A, Packer J, Lin D, Ma YA, Trapnell C. Single-cell mRNA quantification and differential analysis with Census. Nat Methods. 2017;14:309–315. [PubMed: 28114287]
47. Trapnell C, Cacchiarelli D, Grimsby J, Pokharel P, Li S, Morse M, Lennon NJ, Livak KJ, Mikkelsen TS, Rinn JL. The dynamics and regulators of cell fate decisions are revealed by pseudotemporal ordering of single cells. Nat Biotechnol. 2014;32:381–386. [PubMed: 24658644]
48. MacArthur J, Bowler E, Cerezo M, Gil L, Hall P, Hastings E, Junkins H, McMahon A, Milano A, Morales J, et al. The new NHGRI-EBI Catalog of published genome-wide association studies (GWAS Catalog). Nucleic Acids Res. 2017;45:D896–D901. [PubMed: 27899670]
49. Consortium GT, Laboratory DA, Coordinating Center -Analysis Working G, Statistical Methods groups-Analysis Working G, Enhancing Gg, Fund NIHC, Nih/Nci, Nih/Nhgri, Nih/Nimh, Nih/Nida, et al. Genetic effects on gene expression across human tissues. Nature. 2017;550:204–213. [PubMed: 29022597]

Clinical Perspective

What is new?

- Single-cell RNA sequencing results reveal the comprehensive cellular composition and gene expression landscape of control and aneurysmal human ascending aortic wall at the single-cell level.
- Mitochondrial dysfunction present in different aortic cell types may be a feature of ascending thoracic aortic aneurysms (ATAA).
- We identified 11 genes that may be critical for aortic function. Enhancing the activity of the transcription factor ERG in the aorta may be a therapeutic strategy for ATAA.

What are the clinical implications?

- Elucidating the dynamic gene expression in the diverse aortic cell populations of normal and diseased aortas will improve our understanding of the molecular pathogenesis of aortic diseases.
- This information, in turn, will facilitate the development of effective pharmacologic treatment for these conditions.

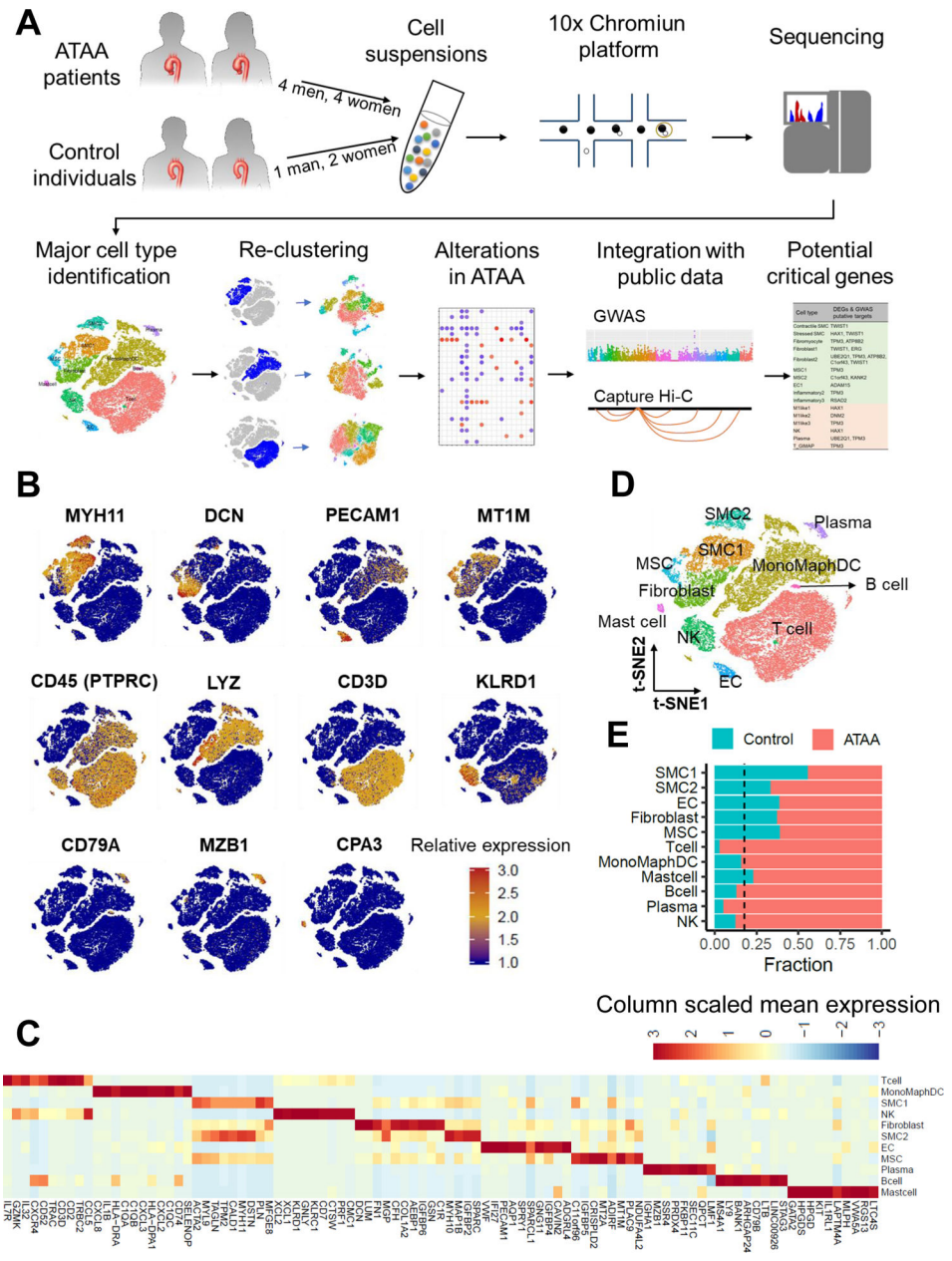

Figure 1. Eleven major cell types identified with sc-RNAseq analysis of human ascending aortic tissues.

A, Experimental approach and data analysis strategy. **B**, Relative expression of several marker genes in all cells from all samples. Cells were projected onto a t-SNE plot. **C,** The mean expression of selected genes in the major cell types. **D**, A t-SNE plot showing all cells colored according to the 11 major cell types. **E**, The composition of each cell type is shown in the horizontal bar plot. The dashed black line represents the expected proportion of cells from the control group (the total number of control cells divided by the total number of cells from all specimens). ATAA indicates ascending thoracic aortic aneurysm; GWAS, genome-wide association studies; MSC, mesenchymal stem cell; SMC, smooth muscle cell; EC,

endothelial cell; MonoMaphDC, monocyte/macrophage/dendritic cell; NK, natural killer cell.

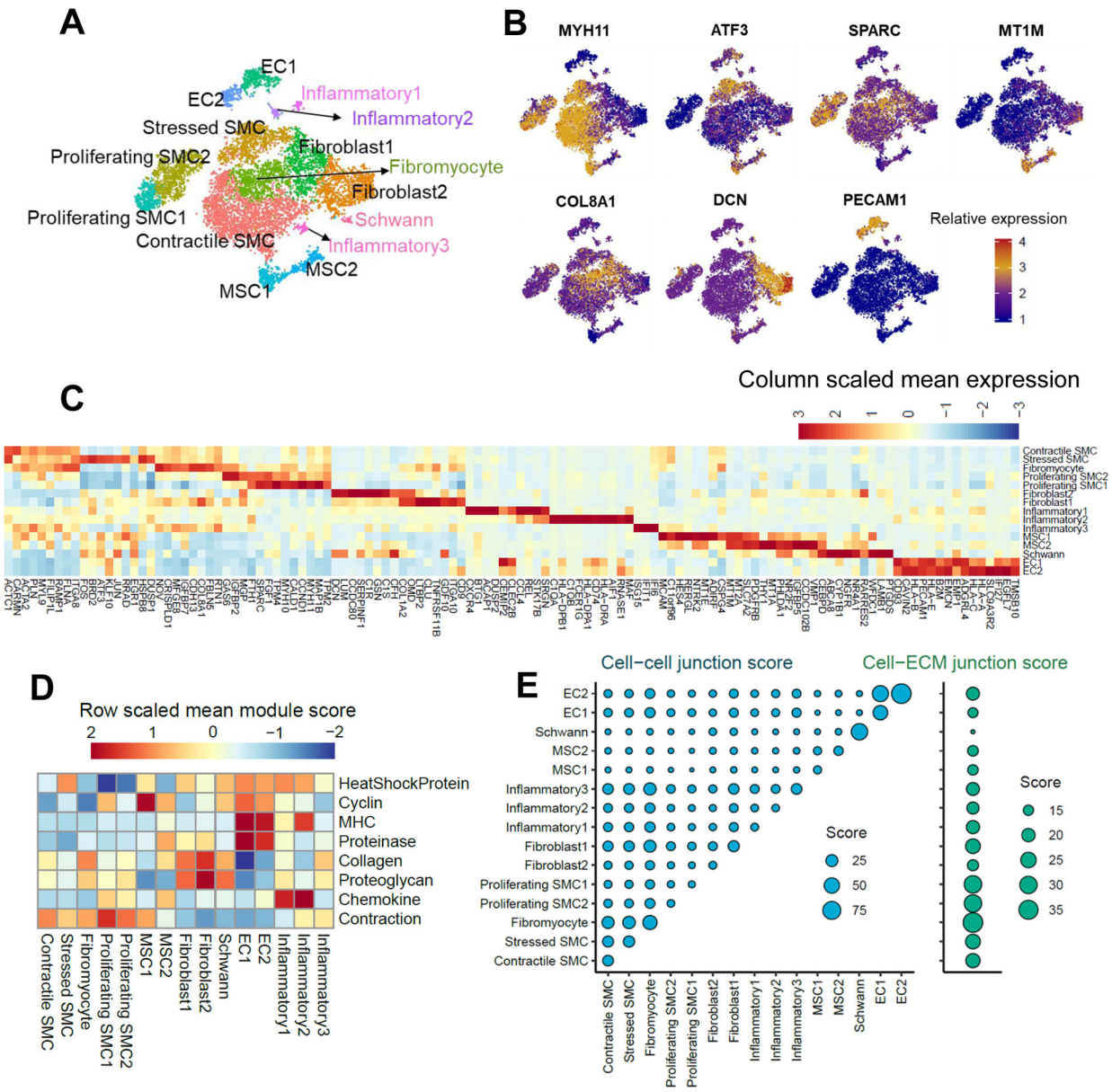

Figure 2. Heterogeneity of nonimmune cells in human ascending thoracic aortic wall.

A, A t-SNE plot of non-immune cells colored according to identified clusters. **B**, Relative expression of several marker genes in nonimmune cells projected onto a t-SNE plot. **C**, Mean expression of select genes in nonimmune cell clusters. **D**, Module scores of 8 features (or functions) in nonimmune cell clusters. **E**, Cell-cell junction scores between nonimmune cell clusters and cell-ECM scores between nonimmune cell clusters and ECM. SMC indicates smooth muscle cell; MSC, mesenchymal stem cell; EC, endothelial cell; MHC, major histocompatibility complex.

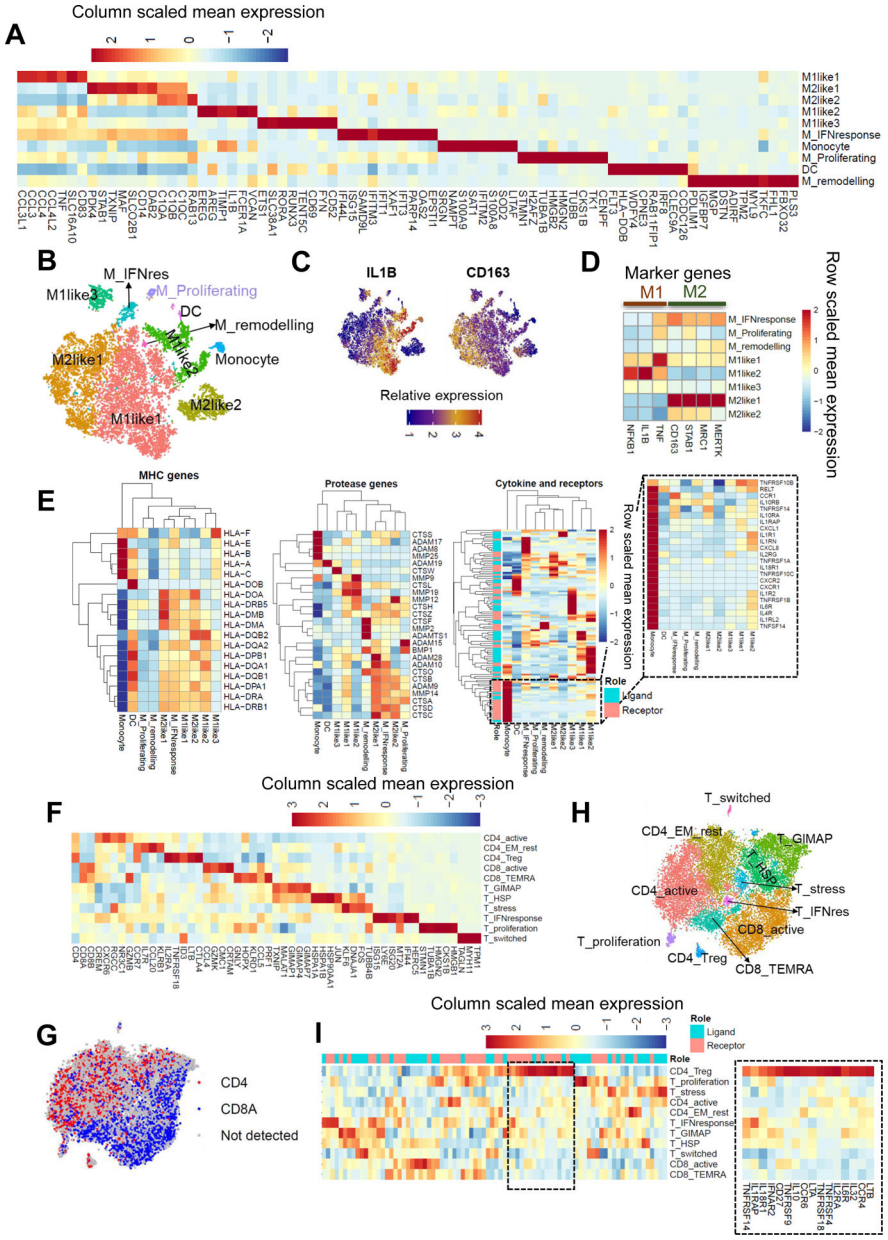

Figure 3. Heterogeneity of immune cells in human ascending aortic tissue.

A, Mean expression of selected genes in monocyte, DC, and macrophage clusters. **B**, A t-SNE plot of all macrophage-like cells colored according to cluster. **C**, Relative expression of *IL1B* and *CD163* in macrophage-like cells projected onto a t-SNE plot. **D**, Mean expression of M1 macrophage and M2 macrophage marker genes in macrophage clusters. **E**, Mean expression of cytokine, proteinase, and MHC genes across macrophage-like cell clusters. Expression values were row scaled and shown by color. Genes with a special expression pattern are shown in a dashed-line box. **F**, Mean expression of selected genes in T lymphocyte cluster. **G**, A t-SNE plot of all T lymphocytes colored according to CD4 and CD8 expression. **H**, A t-SNE plot of all T lymphocytes colored according to cluster. **I**, Mean expression of cytokine genes in T lymphocyte cluster. Genes with a special expression

pattern are shown in a dashed-line box. DC indicates dendritic cell; MHC, major histocompatibility complex.

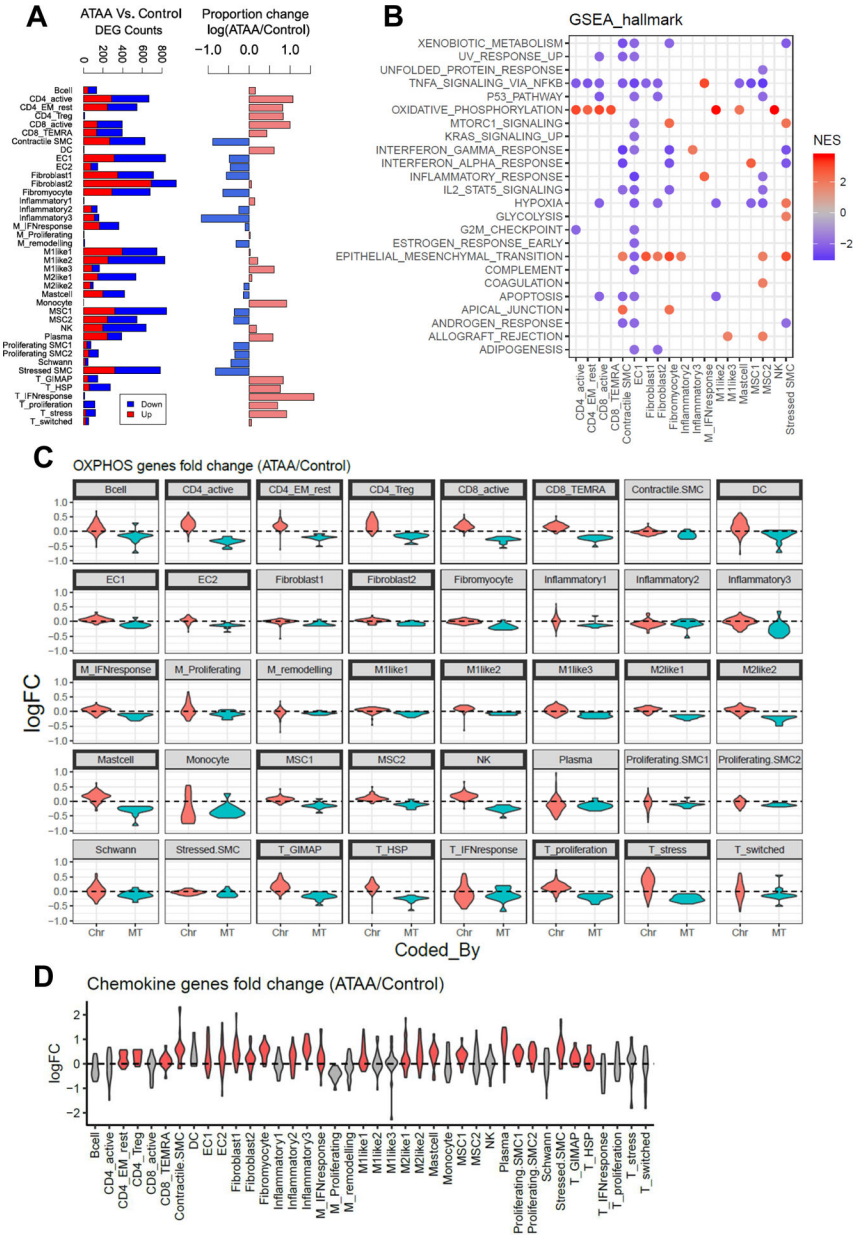

Figure 4. Molecular and cellular alterations in ATAA.

A, Comparison between ATAA and control tissues according to cluster. The x-axis of the left panel represents DEG counts between the ATAA and control groups. Downregulated genes are shown in blue, and upregulated genes are shown in red. The x-axis of the right panel represents the log2-transformed proportion change. The red bar (value > 0) represents the proportion of the cell population increased in ATAA tissues, and the blue bar (value < 0) represents the proportion of the cell population decreased in ATAA tissues. Cell clusters are shown in the y-axis. **B**, Results of GSEA using a hallmark gene set shows enriched DEGs. **C**, Fold change of OXPHOS gene expression (ATAA/control) according to cell cluster. OXPHOS genes were separated according to whether they were chromatin or mitochondrial. Clusters with their names highlighted in a bold black box represent significantly increased

chromatin OXPHOS genes and significantly decreased mitochondrial OXPHOS genes in ATAA tissues. **D**, Fold change in cytokine gene expression (ATAA/control) according to cell cluster. ATAA indicates ascending thoracic aortic aneurysm; DEG, differentially expressed gene; GSEA, gene set enrichment analysis; NES, normalized enrichment score; OXPHOS, oxidative phosphorylation.

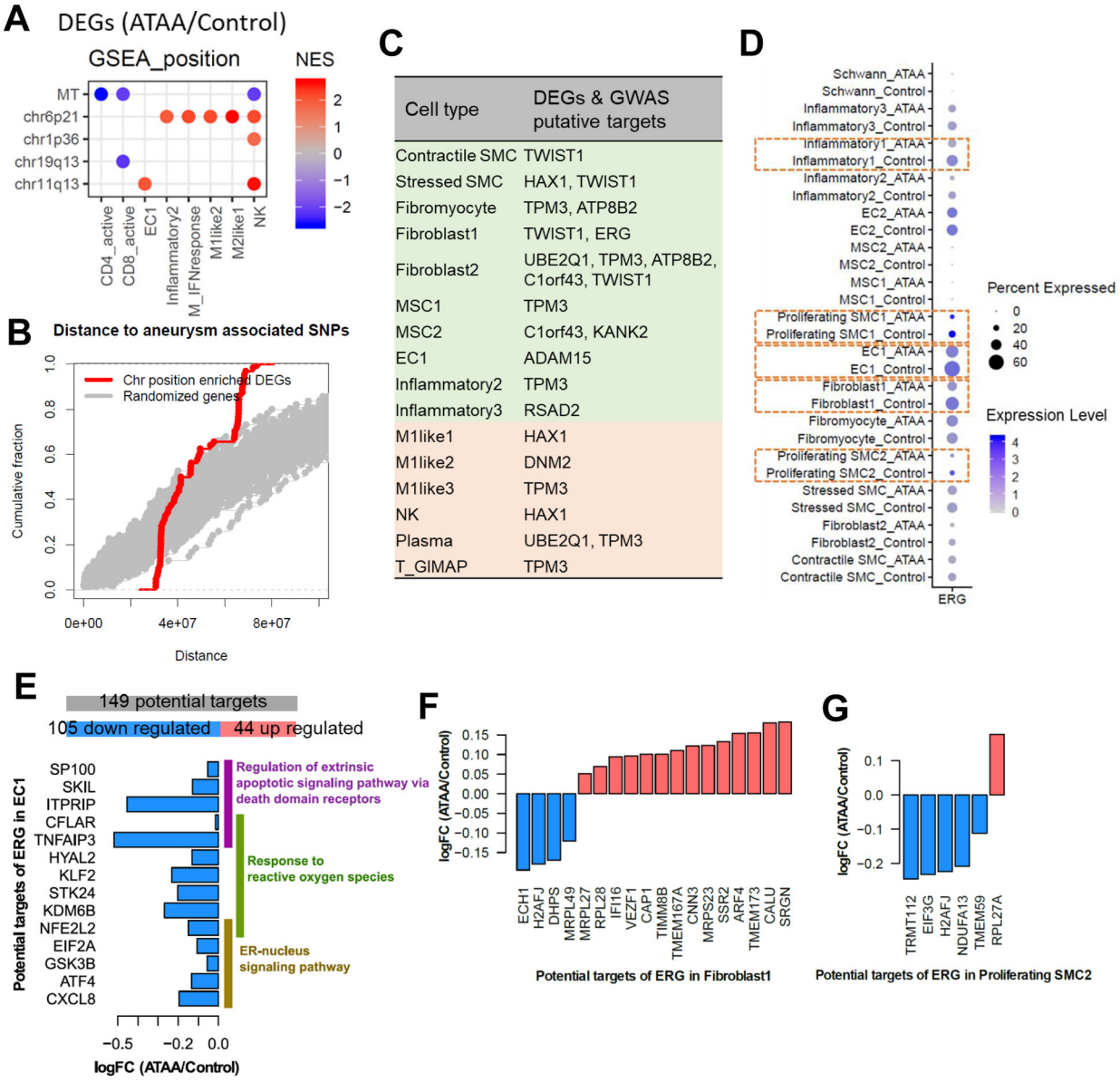

Figure 5. Potential role for *ERG* in SMCs, endothelial cells, and fibroblasts in protecting against aortic aneurysm formation.

A, GSEA position analysis of DEGs. **B**, Distance from chromatin-enriched DEGs (red line) or randomized genes (grey lines) to aneurysm-associated SNPs. **C**, DEGs that were identified as the targets of aneurysm-associated SNPs according to cell cluster. **D**, Expression of ERG in control and ATAA tissues in nonimmune cell clusters. **E**, Potential targets of ERG in EC1. Top, the number of genes identified as potential targets of ERG in EC1. Bottom, the fold-change (ATAA/control) and enriched functions of select potential targets. **F**, Fold-change (ATAA/control) of potential targets of ERG in Fibroblast1. G, Fold-change (ATAA/control) of potential targets of ERG in Proliferating SMC2. GSEA stands for gene set enrichment analysis; NES, normalized enrichment score; SNPs, single nucleotide

polymorphisms; MT, mitochondria; chr, chromatin; DEGs, differentially expressed genes; GWAS, genome-wide association studies; logFC, log10 transformed fold change.

Table 1.

Patient Information for Ascending Aortic Samples (n=11)

Variable	ATAA1	ATAA2	ATAA3	ATAA4	ATAA5	ATAA6	ATAA7	ATAA8	Control4	Control6	Control9
Sex	F	F	M	M	F	F	M	M	F	M	F
Ethnicity	Non-Hispanic	Non-Hispanic	Non-Hispanic	Non-Hispanic	Non-Hispanic	Non-Hispanic	Non-Hispanic	Non-Hispanic	Non-Hispanic	Non-Hispanic	Hispanic
Race	White	White	White	White	White	White	White	White	White	Black	Latino
Age (y)	75	78	59	62	75	67	69	56	63	61	62
Diagnosis/ Comments	ATAA	ATAA	ATAA with root aneurysm	ATAA	ATAA with root aneurysm	ATAA with arch and DTAA	ATAA with root aneurysm	ATAA with root aneurysm	Heart transplant recipient	Heart transplant recipient	Lung transplant donor
Aortic diameter (cm)	5.2	4.9	5	5.2	5.8	4.9	5.2	5.2	NA	NA	2.2
Smoking status	Past (quit before 1990)	Never	Never	Never	Past (quit 1999)	Never	Never	Never	Never	Past	Current
Diabetes	No	No	Yes	Yes	No	No	No	No	No	No	Yes
Hypertension	Yes	Yes	Yes	Yes	Yes	Yes	Yes	Yes	No	Yes	Yes
COPD	No	Yes	No	No	Yes	No	No	No	No	No	No
Aortic valve regurgitation	No	No	Yes	Yes	Yes	Yes	No	Yes	No	No	No
BAV	No	Yes	Yes	No	No	No	NA	No	NA	NA	No
Re-operation	No	No	Yes *	No	No	No	Yes **	No	No	No	No

* Previous arch debranching before stent graft repair of arch and descending thoracic aorta

** Previous aortic valve replacement

ATAA, ascending thoracic aortic aneurysm; BAV, bicuspid aortic valve; COPD, chronic obstructive pulmonary disease; DTAA, descending thoracic aortic aneurysm; F, female; M, male; NA, not available